Macromolecules
ARTICLE

Macromolecules **2010**, *43*, 3785–3793 **3785**
DOI: 10.1021/ma100263k

Spin Capturing with "Clickable" Nitrones: Generation of Miktoarmed Star Polymers

Edgar H. H. Wong,[†,‡] Martina H. Stenzel,[‡] Thomas Junkers,*[,†,§] and Christopher Barner-Kowollik*[,†]

[†]*Preparative Macromolecular Chemistry, Institut für Technische Chemie und Polymerchemie, Karlsruhe Institute of Technology (KIT), Engesserstr. 18, 76128 Karlsruhe, Germany, and* [‡]*Centre for Advanced Macromolecular Design (CAMD), School of Chemical Sciences and Engineering, The University of New South Wales, Sydney, NSW 2052, Australia.* [§]*Current address: Institute for Materials Research (IMO), Universiteit Hasselt, Agoralaan, Gebouw D, 3590 Diepenbeek, Belgium.*

Received February 3, 2010; Revised Manuscript Received March 4, 2010

ABSTRACT: A novel nitrone (α-4-(3-(trimethylsilyl)prop-2-ynyloxy)-*N*-*tert*-butyl nitrone) with an alkyne "click" function is synthesized and employed in enhanced spin capturing polymerization (ESCP) as well as in radical coupling reactions between polymers preformed by atom transfer radical polymerization (ATRP) to generate midchain functionalized polymers. Both techniques allow for the facile introduction of chemical functionalities into a polymer midchain position and hence provide an attractive synthetic avenue for the construction of complex macromolecular architectures. Such a strategy is evidenced by the efficient use of polystyrene and poly(isobornyl acrylate) featuring an alkoxyamine midchain function in polymer−polymer conjugation reactions with azide-terminated polymers, yielding 3-arm star (co)polymers via the Cu-catalyzed alkyne/azide cycloaddition reactions. The successful formation of star-block co- and homopolymers is confirmed by conventional size exclusion chromatography (SEC) as well as via hyphenated liquid absorption chromatography under critical conditions (LACCC)-SEC techniques. The synthetic approach reported herein demonstrates that click functional nitrones can efficiently be employed as macromolecular construction agents in modular reactions.

Introduction

The advent of controlled radical polymerization, CRP,[1−4] has allowed for the preparation of complex polymeric materials of variable composition (e.g., homopolymers, block copolymers) and topologies (e.g., linear, star, brush, comb) with controllable architectures and wide ranging properties under milder conditions than living ionic polymerization.[5,6] In tandem with the application of modular synthetic approaches (*click* chemistry),[7,8] which can be highly efficient for polymer−polymer conjugation reactions,[9−12] there exists a great degree of flexibility in the generation of complex macromolecules. However, despite the availability of these chemistries, the synthesis of such materials often requires multiple strategically designed synthetic pathways and/or chemicals, which may thus not always be easily achievable. Thus, novel procedures and methodologies are continuously developed with the aim of providing less demanding synthetic alternatives toward designing well-defined complex macromolecular architectures.

Recently, we have reported the development of a nonliving CRP technique termed enhanced spin capturing polymerization (ESCP)[13−15] using nitrones as molecular weight control agents based on previous studies concerning thioketone-mediated polymerization[16−19] as well as laser-induced marking of polymer chains in pulsed laser polymerization experiments.[20] In addition, we have also introduced a nitrone-mediated radical coupling reaction for ligating two polymer chains prepared via atom transfer radical polymerization (ATRP).[21] Both ESCP and the radical coupling reaction, although slightly differing from another—the former employs nitrones directly in a polymerization medium while the latter uses nitrones to enforce coupling of two preformed polymeric chains—feature one general commonality: The generation of macromolecules with so-called *midchain* functionalities. Generation of polymers having a functional group in the middle of the polymer chain is rare despite a few recent examples including the cobalt-mediated radical coupling[22,23] method, where dienes act as linkages between two polymeric building blocks preformed by cobalt-mediated radical polymerization. In the case of ESCP the generated alkoxyamine is centered in a midchain position, and the polymer product can be employed in further polymerization reactions via chain extension, for e.g. by nitroxide-mediated polymerization, giving access to triblock copolymer structures.[13,15] In addition, as both the nitroxide formation and radical-based reactions are tolerant toward a large number of functional groups, secondary functionalities such as alkynes can be introduced concurrently into the middle of a polymer chain via the alkoxyamine (derived from the nitrone molecule), thus allowing for post polymer−polymer conjugation reactions. It is this feature that will be exploited and described in detail in the current contribution.

In the present article, we report the synthesis of an *N*-*tert*-butyl-α-phenyl PBN-type nitrone **1** featuring a functional alkyne group that can undergo cycloaddition reactions with an azide-terminated species via the Cu-catalyzed alkyne/azide cycloaddition, CuAAC, reaction.[9,10] Variable derivatives of nitrones have been previously synthesized and applied in polymerization reactions, most notably in the work by Detrembleur and Jerome[24] as well as Grishin and co-workers[25] in their in situ

*Corresponding authors: e-mail christopher.barner-kowollik@kit.edu, Tel +49 721 608 5641, Fax +49 721 608 5740 (C.B.K.); e-mail thomas.junkers@uhasselt.be, Tel +32 11 26 8318, Fax +32 11 26 8399 (T.J.).

Published on Web 03/16/2010

Scheme 1. Spin Capturing of Macroradicals with Alkyne-Bearing Nitrone 1 and the Subsequent Cu-Catalyzed Click Reaction Forming 3-Arm Star (Co)polymers[a]

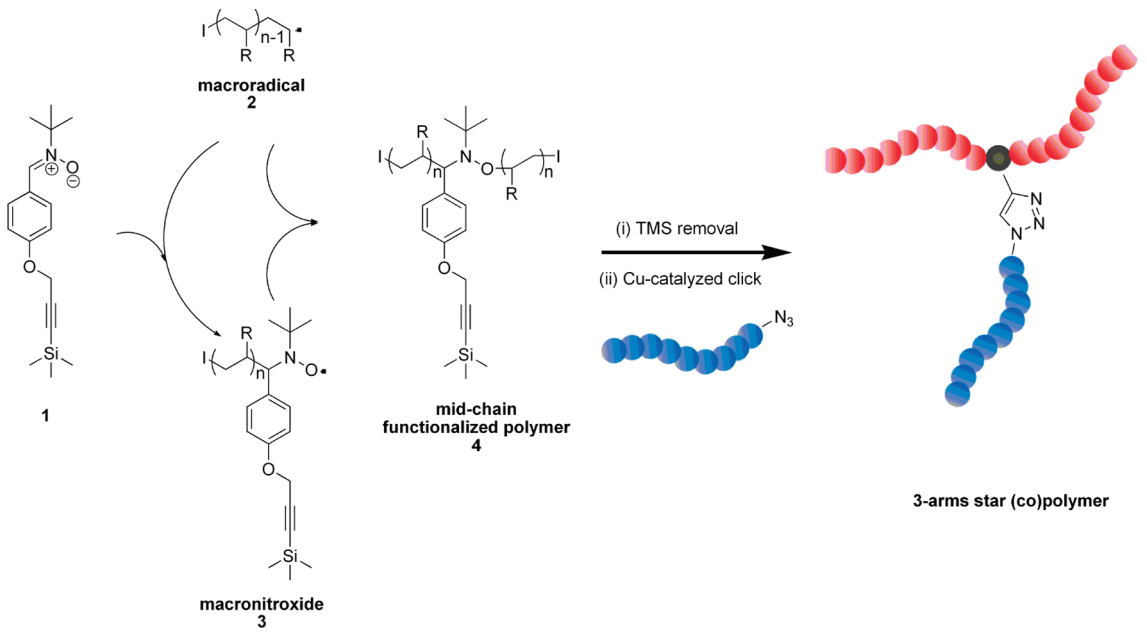

[a] I denotes the polymer end group resulting from the employed initiator, and R represents the monomer side group (COOR for iBoA or phenyl for styrene).

nitroxide-mediated polymerization reactions. However, to the best of our knowledge, the alkyne-bearing nitrone **1** has not previously been prepared and employed in modular polymer synthesis. To demonstrate the utility of the nitrone **1**, polystyrene made from ESCP employing **1** and ATRP-made poly(isobornyl acrylate) that was subjected to the nitrone-mediated radical coupling reaction have been prepared. Both midchain functionalized polymer types were then subsequently coupled to azide-terminated polymers in CuAAC reactions to generate 3-arm star (co)polymers (see Scheme 1).

It is important to note that both the ESCP and radical coupling reactions essentially follow the same reaction mechanism depicted in Scheme 1, where the macroradicals are captured by the nitrone, forming a stable radical spin trap adduct of the macronitroxide species **3** that undergoes an almost immediate second capturing step with another macroradical. However, the key difference between the two methods of preparing midchain functional alkoxyamines lies in the source of the macroradicals: In ESCP, macroradicals are generated during the course of a conventional free radical polymerization process, whereas in the radical coupling reaction the macroradicals are "stored" in the form of the halogenated polymers premade via ATRP and are only released in the presence of a copper/catalyst system. The products from both processes are virtually identical with the ATRP route, however, allowing for polymers with narrow molecular weight distributions. The successful formation of polymers with a distinct midchain positioned alkoxyamine in either technique relies strongly on the fast addition rate of the macroradicals to the nitrone, $k_{ad,macro}$, and the high coupling rate coefficients between macronitroxides and macroradical species.

In the following, the synthesis of midchain functionalized polymers will be presented in detail. The characterization of the formed star (co)polymers will include conventional size exclusion chromatography techniques as well as two-dimensional LACCC-SEC chromatography analysis.

Experimental Section

Materials. 4-Hydroxybenzaldehyde (Aldrich, 98%), propargyl bromide solution (Fluka, 80% in toluene), potassium hydroxide pellets (KOH, Sigma-Aldrich, 85%), dichloromethane (Sigma-Aldrich, 99.9%), magnesium sulfate ($MgSO_4$, Sigma-Aldrich, 97%), silver chloride (Sigma-Aldrich, 99.5%), 1,8-diazabicyclo[5.4.0]undec-7-ene (DBU, Aldrich, 98%), chlorotrimethylsilane (Aldrich, 97%), sodium hydrogen carbonate ($NaHCO_3$, Sigma-Aldrich, 99.7%), *N*-(*tert*-butyl)hydroxylamine acetate (Aldrich, 97%), triethylamine (Sigma-Aldrich, 99%), 2,2-azobis(isobutyronitrile) (AIBN, DuPont), methyl 2-bromopropionate (MBrP, Aldrich, 98%), *N*,*N*,*N*′,*N*″,*N*″-pentamethyldiethylenetriamine (PMDETA, Aldrich, 99%), butyl acetate (Sigma-Aldrich, 99%), copper(II) bromide (Sigma-Aldrich, 99%), copper powder < 75 μm (Cu(0), Aldrich, 99%), toluene (Aldrich, 99.9%), tributyltin hydride (TBTH, Aldrich, 97%), tetrahydrofuran (THF, Sigma, 99%), dimethylformamide (DMF, Aldrich, 99.8%), tetrabutylammonium fluoride trihydrate (TBAF·$3H_2O$, Aldrich, 97%), and sodium azide (Sigma-Aldrich, 99%) were used as received. Styrene (Sty, Aldrich, 99%) and isobornyl acrylate (*i*BoA, Aldrich) monomers were deinhibited by percolating over a column of basic alumina. Copper(I) bromide (CuBr, Sigma-Aldrich, 98%) was washed with glacial acetic acid at 80 °C overnight to remove any soluble oxidized species before being filtered, rinsed with ethanol, and dried.

Synthesis of 4-(Prop-2-ynyloxy)benzaldehyde (5). 4-Hydroxybenzaldehyde (15.14 g, 0.124 mol), KOH (12.3 g, 0.186 mol), and propargyl bromide (27.6 g, 0.186 mol) were weighed into a 100 mL round-bottom flask, and the mixture was dissolved in 60 mL of ethanol and mixed thoroughly. The solution was heated under reflux at 80 °C for 20 h before being allowed to cool down to ambient temperature. Solvent and unreacted propargyl bromide were removed under high vacuum, yielding a dark brown solid. The solid was mixed with water (50 mL) and extracted with diethyl ether (3 × 50 mL). The organic fraction was dried with $MgSO_4$ and filtered, and the solvent was later removed in vacuo. The recovered solids were crystallized in ethanol, yielding brown crystals (yield: 68%, 10.3 g). ^{1}H NMR (300 MHz, $CDCl_3$, 25 °C, δ, ppm): 9.90 (C*H*═O, s, 1H), 7.84−7.87 (Ph, d, 2H), 6.94−6.97 (Ph, d, 2H), 4.78 (O−CH_2−, s, 1H), 2.55−2.57 (−C≡C*H*, t, 1H). ^{13}C NMR (75 MHz, $CDCl_3$, 25 °C, δ, ppm): 191.2 (*C*H═O), 162.8, 132.3, 131.0, 115.6 (Ph), 56.3 (O−*C*H_2−), 78.4 (−*C*≡), 76.7 (≡*C*H).

Synthesis of 4-(3-(Trimethylsilyl)prop-2-ynyloxy)benzaldehyde (6). The trimethylsilyl protection step was adapted from the literature procedure.[26] To a two-neck 100 mL round-bottom flask that contained the aldehyde **5** (7 g, 37.8 mmol) and silver chloride (1.09 g, 7.56 mmol) was first added 60 mL of dry dichloromethane followed by 1,8-diazabicyclo[5.4.0]undec-7-ene (11.5 g, 75.6 mmol). The reaction mixture was then heated under reflux at 40 °C and chlorotrimethylsilane (12.3 g, 113 mmol) added dropwise, and the contents were stirred for 2 days. The mixture was allowed to cool to ambient temperature and diluted with 150 mL of *n*-hexane. The organic phase was subsequently washed successively with aqueous $NaHCO_3$, 2 M HCl, and water before being dried over anhydrous $MgSO_4$, filtered, and concentrated under high vacuum. Beige solids were recovered, and the product was used in the next step without further purification (yield: 89%, 6.2 g). ^{1}H NMR (300 MHz, $CDCl_3$, 25 °C, δ, ppm): 9.88 (C*H*═O, s, 1H), 7.82−7.87 (Ph, d, 2H), 7.05−7.08 (Ph, d, 2H), 4.76 (O−CH_2−, s, 1H), 0.15 (TMS, s, 9H). ^{13}C NMR (75 MHz, $CDCl_3$, 25 °C, δ, ppm): 191.1 (*C*H═O), 162.9, 132.1, 130.8, 115.5 (Ph), 57.1 (O−*C*H_2−), 94.1 (−*C*≡), 99.2 (≡*C*H), −0.08 (TMS).

Synthesis of α-4-(3-(Trimethylsilyl)prop-2-ynyloxy)-*N*-*tert*-butyl Nitrone (1). The aldehyde **6** (6 g, 25.8 mmol), *N*-(*tert*-butyl)hydroxylamine acetate (5 g, 33.4 mmol), and excess $MgSO_4$ (as drying agent to absorb the water byproduct) were weighed into a 250 mL round-bottom flask before dissolving with 100 mL of chloroform. Triethylamine (3.8 g, 33.4 mmol) was added dropwise into the solution. Stirring of the solution at room temperature was stopped after 3 days. Chloroform solvent was removed under high vacuum. Approximately 80 mL of water was added to the flask, and the suspension was extracted with ethyl acetate (3 × 60 mL). The organic fraction was dried with $MgSO_4$ and filtered. Ethyl acetate was removed under high vacuum to yield light yellow solids which were later crystallized in concentrated ethanol, yielding light yellow crystals (yield: 64%, 3.84 g). ^{1}H NMR (300 MHz, $CDCl_3$, 25 °C, δ, ppm): 1.60, (*N-tert* butyl, s, 9H), 7.47 (C*H*═N, s, 1H), 8.27−8.30 (Ph, d, 2H), 6.98−7.01 (Ph, d, 2H), 4.72 (O−CH_2−, s, 1H), 0.15 (TMS, s, 9H). ^{13}C NMR (75 MHz, $CDCl_3$, 25 °C, δ, ppm): 28.7, 70.5 (*N-tert* butyl), 129.7 (*C*H═N), 159.2, 130.9, 125.0, 115.0 (Ph), 57.0 (O−*C*H_2−), 93.5 (−*C*≡), 99.8 (≡*C*H), 0.03 (TMS).

ESCP Reactions. All ESCP reactions are conducted in a similar manner as previously reported in literature.[13−15]

ATRP Reaction. To a 50 mL round-bottom flask containing CuBr (50 mg), *i*BoA (7.5 mL) and MBrP (26 μL) were added, and the solution was degassed by purging with nitrogen for 10 min in an ice bath. A degassed solution of 2.5 mL of butyl acetate with PMDETA (147 μL) was transferred into the flask via a cannula. The reaction mixture was heated at 75 °C in a thermostated oil bath for 30 min, and the polymerization was stopped by immersing the sealed flask in an ice bath before opening to air. A sample was withdrawn from the solution and analyzed by NMR to determine the conversion (∼35% monomer conversion was obtained). The contents in the flask were poured into a beaker containing $CuBr_2$ (150 mg) in THF and was left overnight in high vacuum to remove any solvent and unreacted monomer. Fresh THF was then added to the beaker, and the polymer P*i*BoA **I** was purified by passing the polymer solution over a column of silica gel in order to remove all copper complexes. The copper-free polymer solution was concentrated and subsequently reprecipitated twice in cold methanol, yielding 2.1 g of polymer with M_n = 4300 g mol^{-1} and PDI = 1.21 (by THF-SEC analysis).

Synthesis of PiBoA-N_3. P*i*BoA **I** (430 mg, 100 μmol) was dissolved in a 2 mL mixture of THF:DMF (1:1 volume ratio) before adding an excess of sodium azide (65 mg, 1 mmol). The mixture was stirred for 2 days, and P*i*BoA-N_3 was reprecipitated twice in cold methanol and washed exhaustively with water. ^{1}H NMR and ESI-MS analysis confirmed the formation of the polymer product.

Synthesis of PS-N_3. To a 100 mL round-bottom flask that contains CuBr (143 mg), Sty (50 mL) and MBrP (112 μL) were added, and the solution was degassed by purging with nitrogen for 30 min in an ice bath. Degassed PMDETA (418 μL) was transferred into the flask via a degassed syringe. The reaction mixture was heated at 100 °C in a thermostated oil bath for 40 min, and the polymerization was stopped by immersing the sealed flask in an ice bath before opening to air. A sample was withdrawn from the solution and analyzed by NMR to determine the conversion (∼10% monomer conversion was obtained). The polymer was purified similarly to P*i*BoA **I**, yielding 3.5 g of polymer with M_n = 2700 g mol^{-1} and PDI = 1.14 (by THF-SEC analysis). The bromine-terminated PS-Br was converted to PS-N_3 in identical fashion to P*i*BoA-N_3.

Radical Coupling Reaction. P*i*BoA **I** (860 mg, 200 μmol), nitrone **1** (122 mg, 400 μmol), and Cu(0) (12.8 mg, 200 μmol) were dissolved in 1.6 mL of toluene in a glass vial (to make up a 0.1 M solution of the ATRP polymer) and purged with nitrogen for 10 min in an ice bath. A degassed solution of 400 μL of toluene with PMDETA (43 μL, 200 μmol) was transferred into the glass vial via a degassed syringe. The reaction mixture was heated to 60 °C in an electrical thermomixer for 3 h. The resulting P*i*BoA **II** was purified by passing over a column of silica gel and reprecipitated twice in cold methanol (M_n = 7700 g mol^{-1} and PDI = 1.16 (by THF-SEC analysis)).

Polymer Quenching. P*i*BoA **II** (77 mg, 10 μmol) was dissolved in 538 μL of DMF before adding 2 mmol of TBTH (538 μL) such that the ratio of polymer to quencher is 1:200. The solution was heated to 125 °C for 5 h. Under these conditions, the alkoxyamine bond is cleaved and TBTH transfers its proton to the radicals, preventing recombination. As the hydride is a strong transfer agent, quantitative quenching can be assumed considering the high concentration of the quencher and the relatively high temperature. The solvent was removed by evaporation in a fume cupboard before the quenched polymer was analyzed via THF-SEC (M_n = 5200 g mol^{-1} and PDI = 1.19).

Alkyne Deprotection. The typical procedure for the deprotection of the alkyne is as follows: P*i*BoA **II** (530 mg, 66 μmol) was dissolved in 1 mL of THF. In another glass vial, TBAF·3H_2O (209 mg, 663 μmol) was dissolved in 2.3 mL of THF. Both solution mixtures are purged with nitrogen for 20 min in an ice bath. The solution in the glass vial containing TBAF was transferred to the glass vial containing the polymer solution via a cannula, and the combined mixture was stirred for 24 h at ambient temperature. The resulting P*i*BoA **II** (after TMS removal) was reprecipitated twice in cold methanol. The molecular weight distributions (MWDs) of the polymers before and after TMS removal are almost identical. TBAF, which was used in 10 times excess, allowed for quantitative removal of the TMS group as confirmed by ^{1}H NMR analysis.

Click Reactions. In a general Cu-catalyzed alkyne/azide cycloaddition (CuAAC) reaction, polymers bearing midchain alkyne functionalities (5 μmol) and PS-N_3 (or P*i*BoA-N_3) in a 1:1 mole ratio were dissolved in 1.5 mL of a THF:DMF mixture (2:1 volume ratio) containing CuBr (50 μmol) and were purged with nitrogen for 20 min in an ice bath. PMDETA (50 μmol) was injected into the sealed solution with a degassed syringe, and the reaction mixture was stirred for 48 h at room temperature. The clicked product was purified by passing over a column of silica gel in order to remove all copper complexes. The copper-free polymer solution was concentrated and subsequently reprecipitated twice in cold methanol before any characterization was carried out.

Characterization by THF Size Exclusion Chromatography (THF-SEC). Analysis of the MWDs of the polymer samples were performed on a Polymer Laboratories PL-GPC 50 Plus Integrated System, comprising an autosampler, a PLgel 5.0 μm bead-size guard column (50 × 7.5 mm), followed by three PLgel 5 μm Mixed-C columns (300 × 7.5 mm) and a differential refractive index detector using tetrahydrofuran (THF) as the

Scheme 2. Synthesis of the Nitrone 1[a]

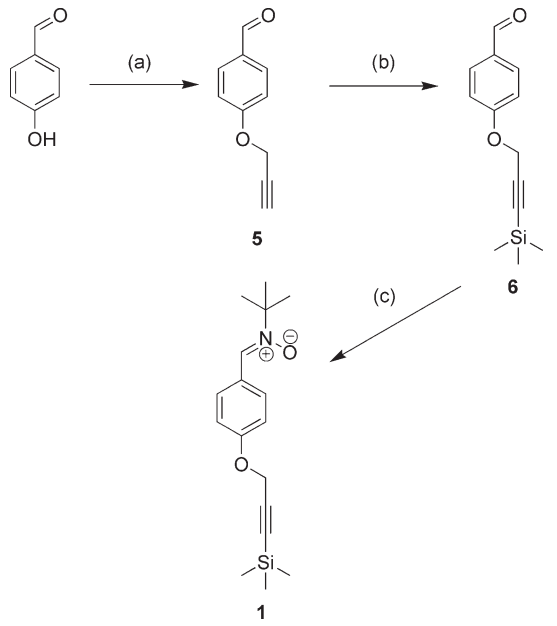

[a] Reactants and conditions: (a) propargyl bromide, KOH, ethanol, reflux at 75 °C, 20 h; (b) chlorotrimethylsilane, AgCl, DBU, dichloromethane, reflux at 40 °C, 2 days; (c) *N*-(*tert*-butyl)hydroxylamine acetate, triethylamine, chloroform, rt, 3 days.

eluent at 35 °C with a flow rate of 1 mL min^{-1}. The SEC system was calibrated using linear narrow polystyrene standards ranging from 160 to 6×10^6 g mol^{-1} (polystyrene ($K = 14.1 \times 10^{-5}$ dL g^{-1} and $\alpha = 0.70$),[27] poly(isobornyl acrylate) ($K = 5.0 \times 10^{-5}$ dL g^{-1} and $\alpha = 0.745$)[28]). Polymer concentrations were in the range of 3−5 mg mL^{-1}.

Characterization by Nuclear Magnetic Resonance (NMR) Spectroscopy. All NMR spectra were recorded on a Bruker DPX spectrometer (300 MHz).

Characterization by 2D LACCC-SEC. Two-dimensional chromatography was carried out on a commercial system from PSS (Mainz). In the first dimension (LACCC), the sample is injected on a C18 LC Column (Agilent Technologies ZORBAX Eclipse XDB-C18) with THF:MeOH = 68:32 as the eluent[29] at a flow rate of 0.1 mL min^{-1}. After passing UV detection (SECcurity GPC1200) samples are transferred via a switch valve onto the second dimension (SEC), which is run on pure THF at a flow rate of 3 mL min^{-1}. SEC separation is achieved by using a high-speed column (SDV, linear M, 20 × 50 mm) provided by PSS. Polymer concentrations are detected via an evaporative light scattering detector (SECcurity ELS4000), and the resulting data are processed using the 2D-module of the WinGPC software.

Results and Discussion

One of the most common procedures to synthesize nitrones is via the condensation of aldehydes or ketones with *N*-monosubstituted hydroxylamines.[30] The commercially available benzaldehyde derivatives with various additional functional groups such as hydroxyl and halides attached to the phenyl ring allow for facile postchemical modifications, making this the method of choice for the synthesis of nitrone **1**. As shown in Scheme 2, the conversion of 4-hydroxybenzaldehyde into nitrone **1** is a straightforward process, where the hydroxyl group was first reacted with propargyl bromide via nucleophilic substitution to introduce the alkyne functionality, followed by the protection of the alkyne with a trimethylsilyl group before finally converting the aldehyde function into a nitrone by reacting with *N*-(*tert*-butyl)hydroxylamine acetate. Over the course of the synthesis, no tedious chromatographic product separation was required, and crystallization procedures were sufficient to ensure high product purity as confirmed by ^{1}H NMR and ^{13}C NMR analysis.

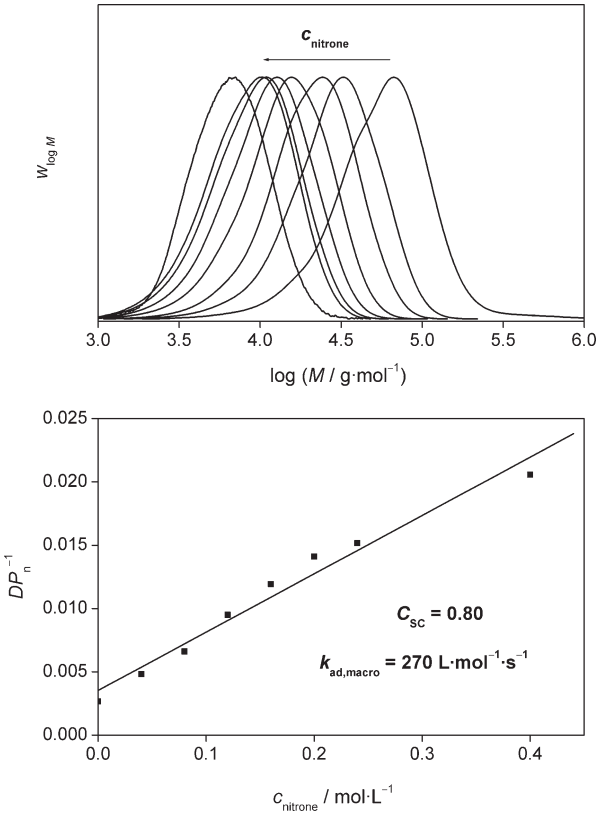

Figure 1. Molecular weight distribution (MWD) of polystyrene samples prepared via ESCP at 60 °C at variable concentrations of nitrone **1** (upper part). The inverse of DP_n is plotted as a function of nitrone concentration for the determination of C_{SC} and $k_{ad,macro}$ in the ESCP of styrene with nitrone **1** (lower part). Note that polymer samples prepared at low monomer conversions (< 5%) are used to determine DP_n.

ESCP and 3-Arm Star Formation. Nitrone **1** is subsequently employed in the ESCP of styrene with 4×10^{-2} mol L^{-1} of the initiator AIBN at 60 °C. The upper part of Figure 1 depicts the molecular weight distribution (MWD) of the polystyrene samples made via ESCP at variable nitrone concentrations, $c_{nitrone}$, while the lower part of the figure shows the plot of the inverse of degree of polymerization, DP_n, of the polystyrene samples as a function of $c_{nitrone}$. Both the upper and lower part of Figure 1 clearly show the polystyrene samples having decreasing molecular weights and DP_n when larger amounts of nitrones are used. Bearing in mind that the ESCP process involves competitive reactions between the macroradicals adding to the nitrone and chain propagation events, at higher nitrone concentrations the propagating chains have a higher tendency to react with the nitrone, thus resulting in shorter chains being captured by the nitrone and the subsequently formed macronitroxide. A satisfactory linear fit is obtained from the plot in the lower part of Figure 1, which is in good agreement with eq 1, where DP_∞ is the DP_n for a conventional radical polymerization (in the absence of nitrones), k_p is the propagation rate coefficient, and c_m is the monomer concentration.

$$DP_n^{-1} = DP_\infty^{-1} + \frac{0.5 k_{ad,\,macro} c_{nitrone}}{k_p c_m} \qquad (1)$$

The results depicted in Figure 1 indeed support the notion that the ESCP mechanism is in place with the new nitrone **1**.

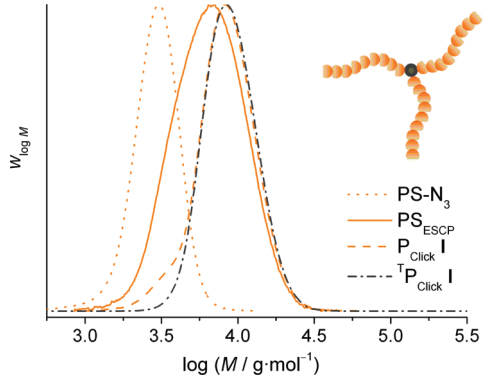

Figure 2. Molecular weight distribution (MWD) of the original polystyrene model compounds PS_{ESCP} and PS-N_3 and the corresponding clicked 3-arm star polystyrene product, P_{Click} **I**. The MWD of the $^{T}P_{Click}$ **I** is a result of the theoretical convolution of the MWD of the starting materials computed via the PREDICI software as described previously.[34]

We have demonstrated earlier that the molecular weights of ESCP-derived polymers can be accurately described by eq 1.[13,14] Since eq 1 bears some resemblance to the Mayo equation for conventional chain transfer polymerization,[31,32] the definition of the spin capturing constant, C_{SC}, was derived for ESCP where $C_{SC} = k_{ad,macro}/k_p$. The C_{SC} of nitrone **1** in the ESCP of styrene at 60 °C is determined to be 0.80 from the slope of the linear fit of the plot in Figure 1 (where c_m of styrene[33] is ~8.3 mol L^{-1}). In order to achieve a constant average molecular weight, M_n, up to high conversions, a C_{SC} value of close to unity is required such that nitrone and monomer are consumed equally over the course of the polymerization. Although not shown explicitly in the present work, the M_n of the polystyrene samples stayed approximately constant up to high monomer to polymer conversions (maximum conversion tested ~50%) since C_{SC} = 0.80 is close to unity. From C_{SC}, $k_{ad,macro}$ can be deduced from the linear fit provided k_p is known. Hence, $k_{ad,macro}$ for the addition of styrenic macroradicals to nitrone **1** is determined to be 270 L mol^{-1} s^{-1} with k_p of styrene[33] at 60 °C being 340 L mol^{-1} s^{-1}. Knowledge of C_{SC} and $k_{ad,macro}$ is important as these numbers allow for a good estimation of target molecular weights in the later synthesis of polymers on a larger scale.

To investigate the formation of 3-arm star polymer, a low molecular weight polystyrene model compound, PS_{ESCP}, which is prepared via ESCP with 4×10^{-1} mol L^{-1} of nitrone **1** (and after deprotection of the alkyne function), is ligated with an azide-terminated polystyrene, PS-N_3, via a CuAAC reaction. Figure 2 shows the MWDs of the polystyrene samples before and after the click reaction. Qualitative analysis of Figure 2 reveals a distinct shift in the molecular weight of the conjugated product, P_{Click} **I**, toward higher molecular weights. Only a small amount of tailing toward the lower molecular weight side is observed which is most likely due to leftover unfunctionalized dead chains from the original bromine-terminated polystyrene made via ATRP that is employed as the precursor in synthesizing PS-N_3. This notion is confirmed by ^{1}H NMR analysis, as the original polystyrene made via ATRP (where the PS-N_3 is derived from) only features 90% bromine functionality. As a result, the following postmodification step in converting from the bromine-terminated polystyrene to the PS-N_3 leads to the loss of at least 10% in azide end-group functionality. Thus, under the assumption that the conjugation reaction does proceed to full conversion, around 10% of "unreacted" material will still be inevitable because the PS-N_3 is contaminated with dead polymeric material from the ATRP process. Also depicted in Figure 2 is the simulated MWD of $^{T}P_{Click}$ **I** as a result of the convolution of the MWD between PS_{ESCP} and PS-N_3 generated via the PREDICI simulation software. Apart from the slight tailing discussed above, almost identical distributions for the theoretical convolution and the experimental SEC trace are found, which is further indication that the formation of the 3-arm star was successful. The simulated MWD in this case (as well as for further examples in the current) gives an estimation on how clicked distributions should look like under perfect conditions and therefore serves as an excellent guideline in assessing the efficacy of polymer−polymer conjugation reactions.[34] It should, however, be noted that the simulations were carried out without assuming column band broadening or hydrodynamic volume effects (caused by the star structure of the polymers under investigation).

Table 1. Peak and Average Molecular Weight Data of the Experimental MWDs Shown in Figure 2

polymer	M_p/g mol^{-1}	M_n/g mol^{-1}	M_w/M_n
PS-N_3	3000	2700	1.14
PS_{ESCP}	7900	5300	1.59
P_{Click} **I**	9400	7400	1.40

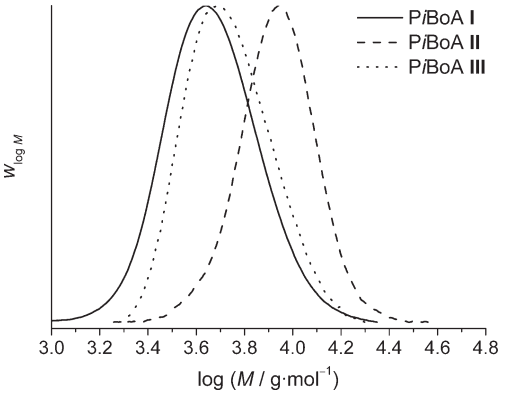

Figure 3. Molecular weight distributions (MWD) of poly(isobornyl acrylate) before nitrone coupling (P*i*BoA **I**), after coupling (P*i*BoA **II**), and after quenching of the alkoxyamine bond (P*i*BoA **III**).

In Table 1, the M_n of P_{Click} **I** approximates the sum of the individual M_n values of 2700 and 5300 g mol^{-1} of PS_{ESCP} and PS-N_3, respectively, which is within the experimental accuracy of the SEC, taking into account the tailing in the MWD of P_{Click} **I**. The shift in MWD together with the systematic increase in the M_n of P_{Click} **I** clearly indicates a successful click reaction and thus the formation of 3-armed star polystyrene.

Radical Coupling Reactions and 3-Arm Star Formations. Another way of generating midchain functionalized polymers in a facile manner (besides ESCP) is by activating preformed ATRP polymers in the presence of a nitrone and a suitable copper/ligand catalyst system. Poly(isobornyl acrylate), P*i*BoA **I** (prepared by ATRP), is reacted with a 2-fold excess of nitrone **1** with Cu(0)/PMDETA at 60 °C for 3 h. During the course of the reaction, macroradicals are freed and reacted with nitrone **1** before coupling with another macroradical, giving access to P*i*BoA **II** bearing an alkyne functionality in its midchain position as described in Scheme 1. The MWDs of the ATRP-made P*i*BoA **I** and the nitrone-coupled P*i*BoA **II** are illustrated in Figure 3. As expected, the molecular weight of the polymer increases due to the coupling reaction.

Collated in Table 2 are the M_n of the SEC traces of the poly(isobornyl acrylate) samples in Figure 3. The doubling of the molecular weight of the ATRP polymer from M_n of 4300 to 7700 g mol^{-1} provides an indication of a successful coupling reaction between the two identical polymer chains. To further prove that a coupling reaction occurred, Figure 4 depicts the full NMR spectra of P*i*BoA **I** and P*i*BoA **II**; the insets show the end- and midgroup regions of these samples. The peak corresponding to the proton in an α-position to the bromine atom in P*i*BoA **I** (**b′**, 4.1−4.3 ppm) quantitatively disappears, and only the end group originating from the ATRP initiator employed in the preparation of the starting polymer (**a′**, 3.5−3.7 ppm) remains in P*i*BoA **II**. Both the SEC and NMR analysis thus confirm that the Br-terminated polymers are reduced and are effectively coupled.

However, the successful coupling reaction by itself does not necessarily indicate that the macroradicals undergo the coupling reaction as described in Scheme 1, as conventional termination by combination of the macroradicals would also lead to similar MWDs as P*i*BoA **II**. Therefore, further analysis of Figure 4 reveals the occurrence of the peak corresponding to the trimethylsilyl protons of the formed alkoxyamine (**c′**, 0.1−0.3 ppm) in PiBoA **II** that is not initially present in PiBoA **I**, supporting the notion that the coupling reaction did in fact proceed via the enhanced spin capturing mechanism. In addition, the ratio of integration of the peaks **c′** to **a′** yields a value of 1.2, which corresponds to ∼90% of midchain functionalization with respect to the nitrone coupling efficiency. To further prove this hypothesis, P*i*BoA **II** is quenched by heating in the presence of a radical scavenger such as tributyltin hydride[15,21] to determine if the nitrone is truly incorporated into the polymer chain: The alkoxyamine centered in the middle of the polymer chain undergoes cleavage at elevated temperatures (> 100 °C). Via the action of the radical scavenger present in the quenching mixture, polymer chains of approximately half of that of the coupled product P*i*BoA **II** should be obtained, i.e., reverting the full distribution back into its original shape (P*i*BoA **I**). The MWD of the quenched product P*i*BoA **III** in Figure 3 shows exactly such behavior as almost the starting distribution of the ATRP polymer P*i*BoA **I** is again obtained after quenching. As can be seen in Table 2, the M_n of P*i*BoA **III** is also similar to that of P*i*BoA **I** within experimental error, although one may assert that the former is marginally higher than the latter. A reasonable explanation for this slight mismatch is that the polymer chains of the quenched sample have an added nitrone **1** unit (with a molecular weight of 303.4 g mol^{-1}) during the coupling reaction, which thus leads to the P*i*BoA **III** having slightly higher molecular weights as compared to P*i*BoA **I**. Despite the slight discrepancy in the M_n between the quenched sample and the original ATRP polymer, it is safe to state that the nitrone-mediated coupling reaction must proceed to a considerable degree, based on the collective results. The generated midchain functionalized

Table 2. Average and Peak Molecular Weight Data of Poly(isobornyl acrylate) Samples (P*i*BoA I−III) Shown in Figure 2

polymer	M_p/g mol^{-1}	M_n/g mol^{-1}	M_w/M_n
P*i*BoA **I**	4200	4300	1.21
P*i*BoA **II**	8700	7700	1.16
P*i*BoA **III**	4700	5200	1.19

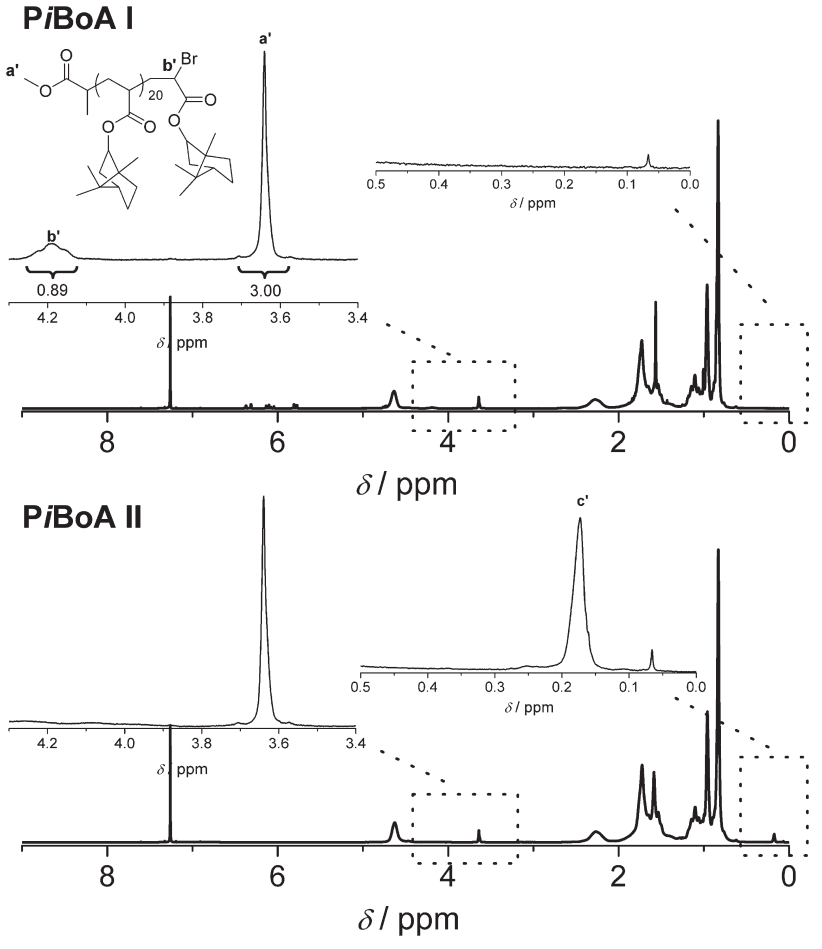

Figure 4. ^{1}H NMR spectra of P*i*BoA **I** and P*i*BoA **II** samples given in Figure 3.

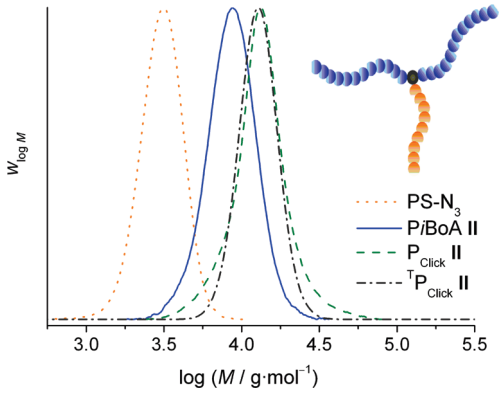

Figure 5. SEC traces of the alkyne bearing polymer, P*i*BoA **II**, azide-terminated polymer, PS-N_3, and the conjugation product, P_{Click} **II**. The theoretical MWD of the conjugate distribution, $^{T}P_{Click}$ **II**, is also included.

Table 3. Peak and Average Molecular Weight Data of the Polymer Samples Shown in Figures 5 and 6

polymer	M_p/g mol^{-1}	M_n/g mol^{-1}	M_w/M_n
PS-N_3	3000	2700	1.14
P*i*BoA-N_3	4200	4300	1.21
P*i*BoA **II**	8700	7700	1.16
P_{Click} **II**	13200	11900	1.19
P_{Click} **III**	12700	10900	1.14

P*i*BoA **II** can therefore be subsequently employed in click reactions to form miktostar structures.

Likewise to PS_{ESCP}, the alkyne function of the P*i*BoA **II** model compound is deprotected prior to the conjugation reaction. Figure 5 depicts the individual SEC traces of the starting polymers, PS-N_3 and P*i*BoA **II**, as well as the experimental and simulated clicked star MWDs, P_{Click} **II** and $^{T}P_{Click}$ **II**. Inspection of Figure 5 shows a monomodal distribution of P_{Click} **II** at higher molecular weights without any pronounced shoulders and only minor tailings toward the lower molecular weight side, which is a good initial indication of a successful click reaction when conjugating two polymer samples of relatively narrow polydispersities (∼PDI < 1.2). When comparing the experimental and theoretical MWDs of the conjugate product, both distributions match well—further proof of a well-working click reaction. The molecular weights of the polymer samples in Figure 5 are listed in Table 3. The M_n of the miktoarm star polymer is in good agreement with the sum of the measured M_n values of the individual starting polymers, all in all strongly pointing toward the successful click reaction and thus the formation of star polymers. When the experimental and theoretical MWDs of the click product are examined, a slightly broader distribution is seen in the experiment compared to the prediction. This tailing to both sides of the distribution may easily be explained by the imperfect separation of block copolymers on a conventional SEC system, which could not be taken into account in the simulation.

In an attempt to provide more evidence on the purported synthesis strategy in the generation 3-arm star (co)polymers, a third reaction involving the ligation between P*i*BoA **II** and another azide-terminated poly(isobornyl acrylate), P*i*BoA-N_3, is performed. Figure 6 depicts the MWDs of the polymer samples involved in this click reaction as well as the theoretical convolution of the starting materials, $^{T}P_{Click}$ **III**. Similar to what is observed in Figures 2 and 5, a monomodal distribution of the clicked product, P_{Click}**III**, occurs at higher molecular weights compared to the starting polymers. The

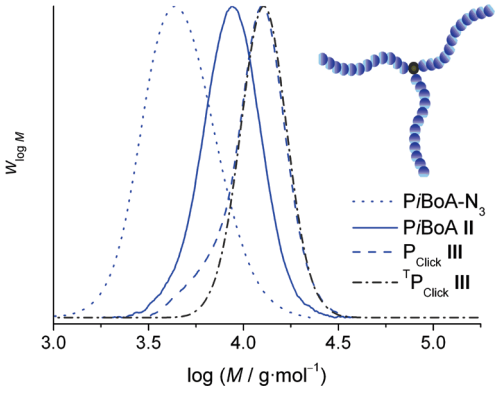

Figure 6. Molecular weight distributions (MWDs) of the poly(isobornyl acrylate) samples, P*i*BoA-N_3, P*i*BoA **II**, and P_{Click} **III**, as well as the simulated distribution of the clicked product, $^{T}P_{Click}$ **III**.

M_n value of 10 900 g mol^{-1} of the star homopolymer is also equivalent to the sum of the M_n of the starting polymers P*i*BoA **II** (M_n = 7700 g mol^{-1}) and P*i*BoA-N_3 (M_n = 4300 g mol^{-1}). In addition, the SEC trace of P_{Click} **III** matches perfectly with the theoretical distribution, although a small tailing is observed in this case, too. The tailing can most probably be attributed to the inherent dead polymers present in the P*i*BoA-N_3 for exactly the same reason as that to the PS-N_3. ^{1}H NMR analysis confirms that only 89% of the polymer chains in P*i*BoA-N_3 are functionalized with the azide end group. Moreover, the same polymer precursor which is used in synthesizing P*i*BoA-N_3, i.e., the ATRP polymer P*i*BoA **I** which has only 89% bromine end groups, is subjected to the nitrone-mediated radical coupling reaction to generate P*i*BoA **II**. Again, the dead chains that are actually present in both P*i*BoA **II** and P*i*BoA-N_3 formed most likely during the ATRP reaction itself (and partially from the radical coupling reaction in the case of P*i*BoA **II**), contributing to the tailing in the distribution of P_{Click} **III**.

2D LACCC-SEC Chromatographic Analysis. Despite the adequacy of conventional SEC techniques in indicating the successful formation of star copolymer via click reactions, it is nonetheless difficult to assess the purity of the copolymer by judging solely from its molar masses since the copolymer distribution also varies in terms of its chemical composition and/or functionality. Hence, chromatographic characterization of copolymers in more than one dimension is required. Two-dimensional LACCC-SEC chromatography is an appropriate tool for such purposes, as it allows for simultaneous yet independent measurement of a polymer's chemical composition and constituting molar mass. The strength of LACCC-SEC has been demonstrated as an analytical procedure allowing for an efficient analysis of block copolymers.[35,36] In LACCC-SEC, polymer mixtures are first solely separated according to their chemical composition in the HPLC dimension, and the respective eluents are then subjected to further separation according to their hydrodynamic volumes by normal SEC.

The critical conditions for poly(isobornyl acrylate) are utilized to perform the analysis in the first dimension under critical conditions. Under such critical conditions, the entropic and enthalpic effects between the poly(isobornyl acrylate) samples and the packing column cancel each other out, and therefore polymers with different molar masses elute at the same retention volume. In other words, the polymers are now no longer separated by size but according to their chemical heterogeneity in the first (LACCC) dimension. Figure 7 shows the 2D chromatograms of the P*i*BoA **II**,

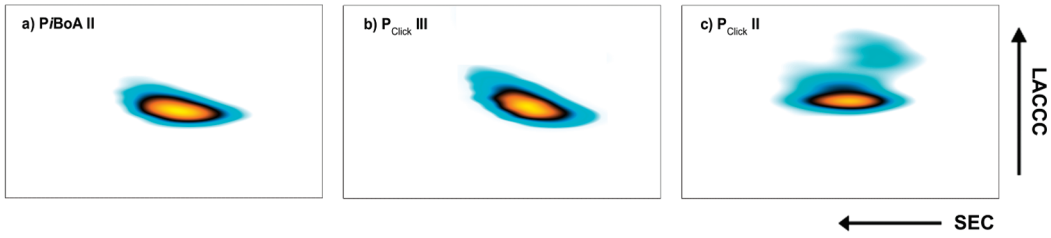

Figure 7. LACCC-SEC chromatograms of P*i*BoA **II** and the subsequent clicked star products. The *y*-axis is the LACCC elution volume (not scaled), and the *x*-axis corresponds to the elution volume in the SEC dimension.

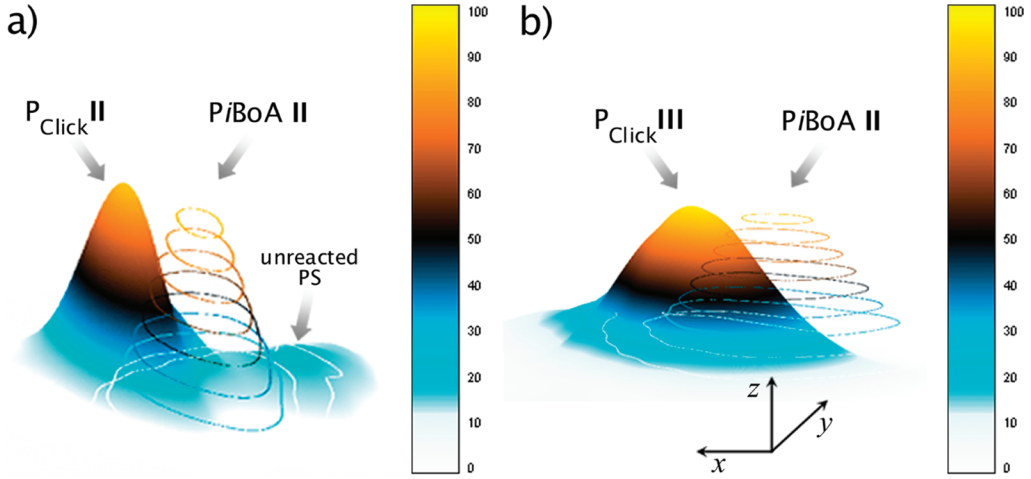

Figure 8. LACCC-SEC chromatograms in 3D view of the overlaps between P*i*BoA **II** with P_{Click} **II** (a) and with P_{Click} **III** (b). The *x*, *y*, and *z* axis correspond to SEC, LACCC and concentration dimensions, respectively.

P_{Click} **II**, and P_{Click} **III** samples. Although the LACCC scales (*y*-axis) of the three chromatograms are not scaled absolutely, a comparison indicates that the peaks of P*i*BoA **II** and P_{Click} **III** are identical, i.e., approximately having the same elution volume. This is in line with the fact that both these samples are composed of the same isobornyl acrylate monomer units and the only difference being in polymer topology and molar masses. Thus, because of the same chemical composition, there is no apparent chemical separation in the LACCC dimension. However, upon comparing P*i*BoA **II** and P_{Click} **II**, a distinctive change in elution volume on the LACCC dimension is observed in which the star copolymer P_{Click} **II** elutes faster compared to the linear homopolymer of P*i*BoA **II**. The additional attachment of the polystyrene block alters the chemical structure of the clicked star, thus allowing for an efficient separation by LACCC analysis. Also observable in Figure 7c is a shoulder peak corresponding to unfunctionalized polystyrene. Integration of the peaks provided quantitative data on the composition of the final clicked product P_{Click} **II**. Unfunctionalized PS that occurs in the chromatogram is close to 10% of the final product, which is in agreement with the aforementioned NMR results that indicated about 10% of dead polymers present in the azide-terminated polystyrene.

For a clearer and more illustrative comparison between the starting polymer P*i*BoA **II** and the formed conjugated products in Figure 7, overlays of their chromatograms are plotted in a 3D view as shown in Figure 8. An additional concentration axis is included into the 2D chromatograms, making the 3D view possible. The results in Figure 8 strengthen the conclusions drawn from Figure 7 as distinguishable distributions between P*i*BoA **II** and P_{Click} **II** on the LACCC scale are obtained, whereas such clear differences are not visible between P*i*BoA **II** and P_{Click} **III**.

Conclusions

The novel compound α-4-(3-(trimethylsilyl)prop-2-ynyloxy)-*N*-*tert*-butyl nitrone **1** was prepared and successfully utilized in ESCP and nitrone-mediated radical coupling reactions to produce polystyrene and poly(isobornyl acrylate), respectively, with alkyne functions in the middle of the polymer chains. The subsequent CuAAC reactions with azide-terminated polymers to form 3-arm star (co)polymers were also successful and their formation pathways were confirmed by conventional SEC techniques as well as 2D LACCC-SEC analysis. The technology developed in the present study, which includes the combination of the relatively facile generation of midchain functionalized polymers via ESCP or radical coupling reactions, together with the efficient orthogonal conjugation reactions lay the foundation for the development of new promising synthetic strategies in the generation of complex macromolecular architectures via nitrone-mediated polymerization processes.

Acknowledgment. C.B.-K. acknowledges funding from the Karlsruhe Institute of Technology (KIT) in the context of the Excellence Initiative for leading German universities, the German Research Council (DFG), and the Ministry of Science and Arts of the state of Baden-Württemberg. T.J. is grateful for support from the Fonds der Chemischen Industrie. E.H.H.W. and C.B.-K. are thankful for a postgraduate scholarship from UNSW central funding. M.H.S. acknowledges a future fellowship from the ARC.

References and Notes

(1) Braunecker, W. A.; Matyjaszewski, K. *Prog. Polym. Sci.* **2007**, *32*, 93–146.
(2) Matyjaszewski, K.; Xia, J. *Chem. Rev.* **2001**, *101*, 2921–2990.
(3) Hawker, C. J.; Bosman, A. W.; Harth, E. *Chem. Rev.* **2001**, *101*, 3661–3688.

(4) Barner, L.; Davis, T. P.; Stenzel, M. H.; Barner-Kowollik, C. *Macromol. Rapid Commun.* **2007**, *28*, 539–559.
(5) Szwarc, M.; Levy, M.; Milkovich, R. M. *J. Am. Chem. Soc.* **1956**, *78*, 2656–2657.
(6) Webster, O. W. *Science* **1991**, *251*, 887–893.
(7) Kolb, H. C.; Finn, M. G.; Sharpless, K. B. *Angew. Chem., Int. Ed.* **2001**, *40*, 2004–2021.
(8) Barner-Kowollik, C.; Inglis, A. J. *Macromol. Chem. Phys.* **2009**, *210*, 987–992.
(9) (a) Altintas, O.; Demirel, A. L.; Hizal, G.; Tunca, U. *J. Polym. Sci., Part A: Polym. Chem.* **2008**, *46*, 5916–5928. (b) Durmaz, H.; Dag, A.; Altintas, O.; Erdogan, T.; Hizal, G.; Tunca, U. *Macromolecules* **2007**, *40*, 191–198.
(10) (a) Tsarevsky, N. V.; Bencherif, S. A.; Matyjaszewski, K. *Macromolecules* **2007**, *40*, 4439–4445. (b) Gao, H. F.; Matyjaszewski, K. *Macromolecules* **2006**, *39*, 4960–4965.
(11) Fournier, D.; Du Prez, F. *Macromolecules* **2008**, *41*, 4622–4630.
(12) (a) Inglis, A. J.; Sinnwell, S.; Davis, T. P.; Barner-Kowollik, C.; Stenzel, M. H. *Macromolecules* **2008**, *41*, 4120–4126. (b) Sinnwell, S.; Inglis, A. J.; Stenzel, M. H.; Barner-Kowollik, C. *Macromol. Rapid Commun.* **2008**, *29*, 1090–1096. (c) Sinnwell, S.; Lammens, M.; Stenzel, M. H.; Du Prez, F.; Barner-Kowollik, C. *J. Polym. Sci., Part A: Polym. Chem.* **2009**, *47*, 2207–2213. (d) Inglis, A. J.; Sinnwell, S.; Stenzel, M. H.; Barner-Kowollik, C. *Angew. Chem., Int. Ed.* **2009**, *48*, 2411–2414.
(13) Wong, E. H. H.; Junkers, T.; Barner-Kowollik, C. *J. Polym. Sci., Part A: Polym. Chem.* **2008**, *46*, 7273–7279.
(14) Wong, E. H. H.; Stenzel, M. H.; Junkers, T.; Barner-Kowollik, C. *J. Polym. Sci., Part A: Polym. Chem.* **2009**, *47*, 1098–1107.
(15) Junkers, T.; Wong, E. H. H.; Stenzel, M. H.; Barner-Kowollik, C. *Macromolecules* **2009**, *42*, 5027–5035.
(16) Ah Toy, A.; Chaffey-Millar, H.; Davis, T. P.; Stenzel, M. H.; Izgorodina, E. I.; Coote, M. L.; Barner-Kowollik, C. *Chem. Commun.* **2006**, 835–837.
(17) Chaffey-Millar, H.; Izgorodina, E. I.; Barner-Kowollik, C.; Coote, M. L. *J. Chem. Theory Comput.* **2006**, *2*, 1632–1645.
(18) Junkers, T.; Stenzel, M. H.; Davis, T. P.; Barner-Kowollik, C. *Macromol. Rapid Commun.* **2007**, *28*, 746–753.
(19) Günzler, F.; Junkers, T.; Barner-Kowollik, C. *J. Polym. Sci., Part A: Polym. Chem.* **2009**, *47*, 1864–1876.
(20) Junkers, T.; Wong, E. H. H.; Szablan, Z.; Davis, T. P.; Stenzel, M. H.; Barner-Kowollik, C. *Macromol. Rapid Commun.* **2008**, *29*, 503–510.
(21) Wong, E. H. H.; Boyer, C.; Stenzel, M. H.; Barner-Kowollik, C.; Junkers, T. *Chem. Commun.* **2010**, DOI: 10.1039/b925390d.
(22) Debuigne, A.; Jerome, C.; Detrembleur, C. *Angew. Chem., Int. Ed.* **2009**, *48*, 1422–1424.
(23) Debuigne, A.; Poli, R.; De Winter, J.; Laurent, P.; Gerbaux, P.; Dubois, P.; Wathelet, J.-P.; Jerome, C.; Detrembleur, C. *Chem.—Eur. J.* **2010**, *16*, 1799–1811.
(24) (a) Sciannamea, V.; Jerome, R.; Detrembleur, C. *Chem. Rev.* **2008**, *108*, 1104–1126. (b) Sciannamea, V.; Catala, J.-M.; Jerome, R.; Detrembleur, C. *J. Polym. Sci., Part A: Polym. Chem.* **2007**, *45*, 1219–1235. (c) Sciannamea, V.; Guerrero-Sanchez, A.; Schubert, U. S.; Catala, J.-M.; Jerome, R.; Detrembleur, C. *Polymer* **2005**, *46*, 9632–9641. (d) Sciannamea, V.; Catala, J.-M.; Jerome, R.; Jerome, C.; Detrembleur, C. *J. Polym. Sci., Part A: Polym. Chem.* **2009**, *47*, 1085–1097.
(25) Kolyakina, E. V.; Grishin, D. F.; Russ *Chem. Rev.* **2009**, *78*, 535–568.
(26) Wiltshire, J. T.; Qiao, G. *J. Polym. Sci., Part A: Polym. Chem.* **2009**, *47*, 1485–1498.
(27) Strazielle, C.; Benoit, H.; Vogl, O. *Eur. Polym. J.* **1978**, *14*, 331–334.
(28) Gruendling, T.; Junkers, T.; Guilhaus, M.; Barner-Kowollik, C. *Macromol. Chem. Phys.* **2010**, *211*, 520−528.
(29) Schmid, C.; Falkenhagen, J.; Barner-Kowollik, C., unpublished results.
(30) Grigoťev, I. A. In *Nitrile Oxides, Nitrones and Nitronates in Organic Synthesis*; Feuer, H., Ed.; Wiley & Sons: New York, 2008.
(31) Odian, G. In *Principles of Polymerization*; Wiley-Interscience: New York, 2004.
(32) Barner-Kowollik, C.; Vana, P.; Davis, T. P. In *Handbook of Radical Polymerization*; Matyjaszewski, K., Davis, T. P., Eds.; Wiley-Interscience: New York, 2002.
(33) Buback, M.; Gilbert, R. G.; Hutchinson, R. A.; Klumpermann, B.; Kuchta, F.-D.; Manders, B. G.; O'Driscoll, K. F.; Russell, G. T.; Schweer, J. *Macromol. Chem. Phys.* **1995**, *196*, 3267–3280.
(34) Barner-Kowollik, C. *Macromol. Rapid Commun.* **2009**, *30*, 1625–1631.
(35) (a) Li, M.; Jahed, N. M.; Min, K.; Matyjaszewski, K. *Macromolecules* **2004**, *37*, 2434–2441. (b) Min, K.; Gao, H.; Matyjaszewski, K. *J. Am. Chem. Soc.* **2005**, *127*, 3825–3830.
(36) Falkenhagen, J.; Much, H.; Stauf, W.; Muller, A. H. E. *Macromolecules* **2000**, *33*, 3687–3693.